

One-dimensional turbulence (ODT): computationally efficient modeling and simulation of turbulent flows

Victoria B. Stephens, David O. Lignell*

Chemical Engineering Department, Brigham Young University, Provo, UT 84602, USA

Abstract

Write this last. About 100 words.

Keywords: turbulence, reacting flows, one-dimensional turbulence

Code Metadata

Nr.	Code metadata description	Please fill in this column
C1	Current code version	1.0
C2	Permanent link to code/repository used for this code version	<i>github.com/BYUignite/ODT</i>
C3	Code Ocean compute capsule	N/A
C4	Legal Code License	MIT
C5	Code versioning system used	Git
C6	Software code languages, tools, and services used	C++, Python 3.x, Yaml,
C7	Compilation requirements, operating environments & dependencies	CMake 3.12+, Cantera, Git, Doxygen (optional)
C8	If available Link to developer documentation/manual	N/A
C9	Support email for questions	davidlignellbyu.edu

Table 1: Code metadata (mandatory)

1. Motivation and significance

Turbulent flows characterize the vast majority of fluid flows in practical engineering applications, and simulations of turbulent flows provide re-

*Corresponding author.

Email address: davidlignell@byu.edu (David O. Lignell)

4 searchers with valuable insights into complex systems, particularly reacting
5 turbulent flows such as combustion processes. Turbulence is a complex phe-
6 nomenon that affects the full range of a flow’s length and time scales. As a
7 result, resolving the entire flow field by numerically solving the Navier-Stokes
8 equations of fluid flow, as is done in direct numerical simulations (DNS), re-
9 quires substantial computational resources. DNS is a powerful research tool,
10 but its high computational cost makes it intractable for simulating most
11 practical engineering flows. In order to achieve numerical solutions to prac-
12 tical flow problems, researchers can use alternative frameworks that model
13 turbulence rather than resolving it directly.

14 Large-eddy simulations (LES) address the problem of wide-ranging length
15 and time scales by combining direct resolution of grid-scale quantities, as in
16 DNS, with subgrid modeling of smaller turbulence structures. The more
17 complex the flow, the more modeling is required; for example, a jet flame
18 simulation might require subgrid modeling for the combustion chemistry, ra-
19 diative heat transfer, or soot chemistry in addition to turbulence structures,
20 all of which form a tightly coupled system in which each model interacts
21 heavily with the others. While subgrid modeling makes LES more computa-
22 tionally affordable than DNS, it can introduce empiricism into simulations,
23 which can lead to inaccurate results. Additionally, unresolved quantities are
24 often parameterized in state space with empirical relationships or assumed
25 distributions that lack universal applicability. LES is a valuable simulation
26 tool, but its approach to turbulence modeling can introduce unwanted em-
27 piricism and make errors difficult to isolate and quantify.

28 The one-dimensional turbulence model (ODT) functionally reverses the
29 LES approach, modeling large-scale turbulent advection and directly resolv-
30 ing small-scale flow structures, simulating the full range of length and time
31 scales in a single dimension. Because large-scale structures are much easier
32 to study and model than small-scale structures, ODT mitigates or sidesteps
33 many of the subgrid modeling issues that complicate LES. Previous stud-
34 ies show that ODT can attain accuracy comparable to DNS at a fraction
35 of the computational cost [1, 2], making it an attractive tool for simulating
36 turbulent flows. Because the ODT model is one-dimensional, it is limited to
37 homogeneous or boundary-layer flows, such as jets, wakes, and mixing layers;
38 these types of flows, however, are common in nature and central to turbu-
39 lence research. ODT’s computational efficiency and resolution of a full range
40 of scales make it a valuable tool that complements experimental studies and
41 other simulation tools like DNS and LES.

42 Early applications of ODT focused on homogenous turbulence, wakes, and
43 mixing layers [3, 4, 5]. Later extension to variable-density flows and a spatial
44 downstream coordinate system facilitated its growth and application to more

complex flows, including combustion in jet flames [6, 7, 8, 9, 10, 11, 12, 13], counterflow flames [14], wall fires [15], and sooting flames [1, 16, 17, 18, 19], as well as other particle flows [20, 21, 22, 23]. ODT has also served to complement LES through subgrid modeling studies [24, 25, 26] and has been applied to various other flow configurations such as double-diffusive interfaces [27], Rayleigh-Taylor mixing [28], and stratified turbulence [29]. Most recently, the ODT code was extended to include cylindrical and spherical coordinate systems [30, 31, 32].

During the recent implementation of the cylindrical and spherical model formulations, the ODT code was drastically overhauled and reorganized, resulting in its current configuration. The ODT code presented here is a pared down version of the development code, representing the fundamental aspects of the ODT model and its most reliable functions. The example cases in Section 3 are a representative sample of the ODT code’s capabilities as it is presented here. Future releases will expand this code’s functionality with additional features currently in development.

2. Software description

2.1. Model description

The ODT model is described in detail in the literature [3, 5, 33, 30, 34]; only a brief explanation will be given here. In ODT, turbulent advection is modeled with stochastic processes called eddy events, which punctuate the solution of unsteady, one-dimensional transport equations for mass, momentum, and enthalpy. The ODT code uses a Lagrangian finite-volume formulation for diffusive advancement in which mass stays constant within each grid cell while cell volumes increase or decrease according to cell dilation via an adaptive mesh refinement [34].

Transport equations for mass, momentum, and enthalpy in the temporal formulation of ODT take the following generic form, derived from the Reynolds Transport Theorem [35] for a given scalar quantity per unit mass β :

$$\frac{d\beta}{dt} = -\frac{j_{\beta,e}A_{x,e} - j_{\beta,w}A_{x,w}}{\rho V} + \frac{S_{\beta}}{\rho V}. \quad (1)$$

Here, j_{β} is the diffusion flux of scalar β across the cell face area A_x where the subscripts e and w refer to the "east" and "west" faces of the grid cell, respectively. S_{β} is the Lagrangian source term derived from the conservation law for β , ρ represents mass density, and V represents cell volume. In practice, we refer to the left hand term on the right side of Equation 1 as the "mixing term" and the right hand term on the right side of Equation 1 as the "source term". The generic transport equation differs slightly in the spatial

formulation of ODT, but its form is the same, so we omit it here for brevity. The system of ordinary differential equations (ODEs) that results is well behaved at all grid points and in all geometries in their finite-volume forms. For details on transport equation derivation and use in both the temporal and spatial formulations of ODT, see Lignell et al. [30].

Eddy events occur as a Poisson process in accordance with their eddy rates, where a given eddy event of size l and location x_0 has an eddy timescale t and an associated eddy rate $1/t$. Three user-defined ODT parameters control the eddy event process: the eddy rate parameter C scales the rate of occurrence of the eddies; the viscous penalty parameter Z suppresses small eddies; and the large eddy suppression parameter β constrains eddies such that they do not reach over the elapsed simulation time. Sampled eddies that do not fit the defined parameters are rejected and not applied to the domain.

Eddy events modify domain variables using triplet maps, as illustrated for a cylindrical domain in Figure 1. For a region of eddy size l , the domain is copied to create three map images; the three images are then placed back to back with the middle image inverted to maintain continuity, and the composite is reapplied to the domain. This process applies to all transported variables on the domain. Applied properly, the triplet map increases scalar gradients and decreases length scales consistent with the application of turbulent eddies in real flows, conserves all quantities and their statistical moments, and maintains continuity in property profiles. Subsequent eddies in the same region will result in a cascade of scales, and eddy rates depend on eddy size and the local kinetic energy such that they follow turbulent cascade scaling laws.

Eddy events occur concurrently with diffusive advancement via solution of the system of unsteady one-dimensional transport equations. In this way, the ODT code marches in time or space until it reaches its end point. Due to the stochastic nature of eddy events, each ODT simulation, or realization, is different, even when it is provided with the same input parameters. In order to obtain statistically stable data for a given set of parameters, we run many realizations with the same input parameters and time-average them. This is done via post-processing tools, which are provided in the ODT package.

2.2. Software Architecture

The ODT package consists primarily of an object-oriented C++ code responsible for running flow simulation cases and generating data. The package also contains auxiliary data processing and visualization tools, written mostly in Python. The post-processing tools are case-specific but will be addressed in Section 2.3.

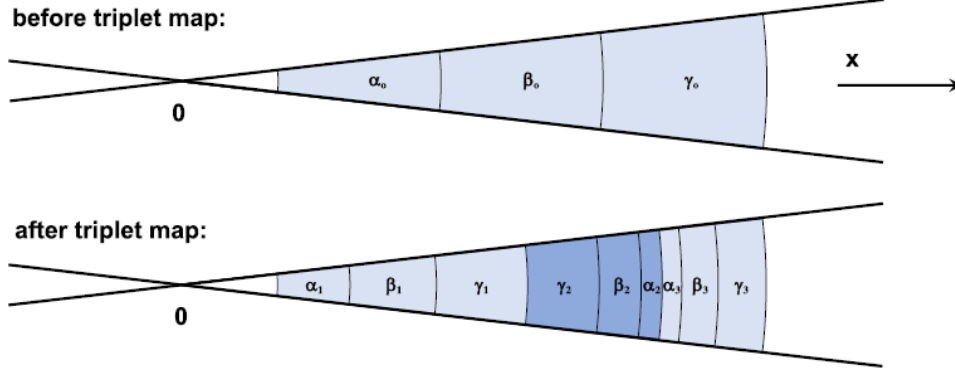


Figure 1: Schematic diagram of a cylindrical triplet map, adapted from [30]. Before the triplet map, the domain contains three grid cells of equal volume, while after the triplet map has been applied, the domain contains nine cells. The nine final cells are labeled according to the cells from which they originated and shaded to indicate that three map images were combined to create the final composite.

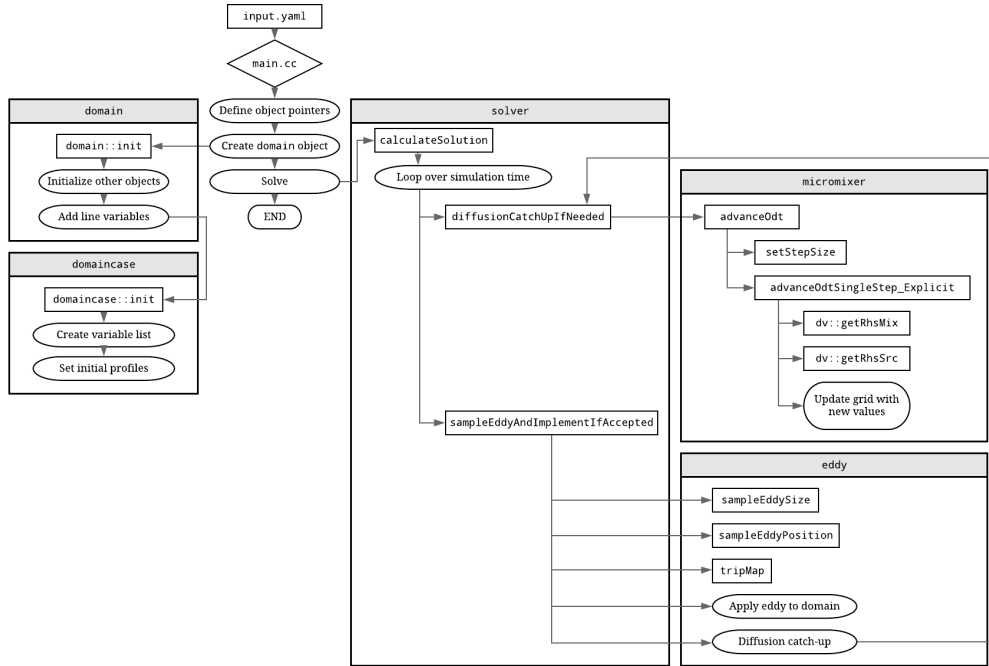


Figure 2: Basic structure of the ODT code. For clarity and brevity, this diagram makes two major assumptions: first, that diffusion advancement in the `micromixer` uses an explicit solution method; and second, that the eddy event sampled by the `eddy` object passes all rejection tests before being applied to the domain.

Figure 2 illustrates the ODT code’s most important objects and structural features. User inputs are provided to the executable in YAML [36] format via `input.yaml`; the location of the specific `input.yaml` file to be used is determined by the case name and case type specified in the run script. The `main` function defines storage for the main objects, but, once created, the `domain` object is responsible for object initialization as well as variable initialization and storage via a case-specific `domaincase` object.

Three primary objects handle the code’s main functions: the `solver`, `micromixer`, and `eddy` objects. The `solver` coordinates the ODT solution process, marching along the simulation time and invoking diffusive advancement and eddy events when appropriate. The `micromixer` handles diffusive advancement by setting step sizes, interacting with the transported domain variables, and solving the system of ODEs defined by Equation 1 (or its equivalent in the spatial formulation). The `micromixer` includes three solution methods that can be specified in `input.yaml`, each appropriate for various case types: a first-order explicit Euler method (pictured in Figure 2); a first-order semi-implicit method that uses CVODE [37] to advance coupled ODEs in individual grid cells, integrated sequentially; and a second-order Strang splitting method [38] good for treating stiff chemistry. In reacting flow cases, chemical kinetics are handled by Cantera [39], which uses transported variable values—enthalpy and gas species composition, for instance—to specify local scalar values such as gas temperature or density, which can affect flow properties. The `micromixer` is also the code’s primary point of interaction with the `mesher` object (not pictured in Figure 2), which manages the adaptive grid functions. Finally, the `eddy` object manages eddy event selection and implementation, which proceeds as described in Section 2.1.

2.3. Workflow

Within the main download package, several directories organize the ODT package. The `source`, `build`, and `run` directories contain the ODT source code, compilation tools, and run scripts, respectively. The `input` directory contains subdirectories corresponding to several possible case types, each populated with an appropriate input files. The `data` directory, initially empty, holds the raw data files and runtime information generated by ODT, as well as post-processed data files generated from within the `post` directory. Finally, the `doc` directory contains documentation optionally generated by Doxygen [40] during the build process.

DETAILS GO HERE

159 3. Example Cases

160 3.1. Pipe Flow

161 First, we present an incompressible pipe flow simulation using the tempo-
162 ral, cylindrical ODT formulation. Results for three different friction Reynolds
163 numbers ($Re_\tau = 550, 1000, 2000$) are compared to DNS results from El
164 Khoury et al. [41] ($Re_\tau = 550, 1000$) and Chin et al. [42] ($Re_\tau = 2000$) for a
165 pipe diameter of $D = 2.0$ m and flow density of $1.0 \text{ kg}\cdot\text{m}^{-3}$. Friction velocity
166 values of $1 \text{ m}\cdot\text{s}^{-1}$ ($Re_\tau = 550, 1000$) and $2 \text{ m}\cdot\text{s}^{-1}$ ($Re_\tau = 2000$) were assumed
167 and used to calculate the mean pressure gradient driving the flow. Using
168 initial conditions with uniform velocity profiles, simulations were run until a
169 state of developed flow was achieved, at which point data were gathered until
170 statistical convergence for the root mean square (RMS) velocity difference
171 from the mean profiles occurred.

172 The simulations were performed with ODT parameters $C = 5$ and $Z =$
173 350 for the temporal ODT formulation. The values of C and Z were adjusted
174 to give good agreement of the ODT results compared to the DNS. Schmidt
175 et al. [25] showed that higher Z results in the buffer-layer being located
176 further from the wall, and increasing C results in a lower slope of the mean
177 streamwise velocity in the log-layer.

178 RESULTS AND PLOTS GO HERE

179 3.2. Non-reacting Jet

180 Here, we present ODT simulation results for a non-reacting round, tur-
181 bulent jet compared to the experimental data of Hussein et al. [43]. The
182 jet consists of air issuing into air through a 1 in (0.0254 m) diameter duct
183 with a uniform exit velocity of $56.2 \text{ m}\cdot\text{s}^{-1}$ and a reported Reynolds num-
184 ber of 95,500. The ODT simulations use this diameter and velocity with a
185 kinematic viscosity of $1.534 \cdot 10^{-5} \text{ m}^2\text{s}^{-1}$, resulting in a Reynolds number
186 of 93,056. The initial velocity profile in the ODT simulations is a modified
187 top-hat profile in which a hyperbolic tangent function of width $\delta = 0.1D$ is
188 used on either side of the jet to smooth the transition between the jet and
189 the free stream. In the spatial formulation of ODT, the streamwise velocity
190 must be positive everywhere on the line, so a small minimum velocity of
191 $v_{min} = 0.1 \text{ m}\cdot\text{s}^{-1}$ is specified and added across the entire velocity profile.

192 ODT simulations were performed with parameters $C = 5.25$, $\beta_{LES} = 3.5$,
193 and $Z = 400$. The value of Z is the same as the spatial simulations in [15],
194 and the values of C and β_{LES} were adjusted to give good agreement with
195 the experimental data. Note the close agreement of the C and Z parameters
196 here to the optimal values used for the pipe flow simulations ($C = 5$ and
197 $Z = 350$). This illustrates a level of robustness in the ODT parameters

198 and suggests that intermediate values could be successfully applied in both
 199 configurations.

200 1024 independent ODT realizations were performed and results were en-
 201 semble averaged. All quantities are normalized consistent with jet similarity
 202 scaling. Downstream locations are normalized by the jet diameter D , and ra-
 203 dial locations are normalized by $(y - y_0)$, where y is the downstream location
 204 and $y_0 = 4D$ is the virtual origin used in [43].

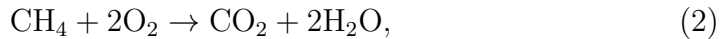
205 RESULTS AND PLOTS GO HERE

206 3.3. Jet Flame

207 ODT is uniquely suited for reacting flow simulations. Here, we present
 208 illustrative ODT simulation results of a round, turbulent jet flame based on
 209 and compared to the experimental DLR-A flame of Meier et al. [44]. This
 210 canonical flame configuration has been used extensively to study and validate
 211 turbulent combustion models [45, 46, 47, 48, 49, 50].

212 The DLR-A fuel stream is mixture of 22.1% CH_4 , 33.2% H_2 , and 44.7%
 213 N_2 (by volume) that issues into dry air via a nozzle with an inner diameter
 214 of 8 mm at a mean exit velocity of $42.2 \text{ m}\cdot\text{s}^{-1}$. The coflow air stream issues
 215 from a concentric nozzle 140 mm in diameter at a velocity of $0.3 \text{ m}\cdot\text{s}^{-1}$. The
 216 reported jet Reynolds number is 15,200.

Previous ODT studies of turbulent jet flames have used the temporal
 planar formulation, but the spatial cylindrical formulation developed recently
 [30] more closely matches the experimental configuration. This simulation
 uses the experimentally reported velocity profiles and jet dimensions. In
 the non-reacting case, a small minimum velocity was added uniformly to
 the velocity profile; no such addition is required here because of the slow-
 moving coflow air stream that issues alongside the reacting jet. The fuel
 was diluted with N_2 in the experimental flame to minimize radiative heat
 losses, and radiation is ignored in the simulation. This flame has a low
 Reynolds number, and the combustion chemistry proceeds quickly. The ODT
 simulation transports the chemical species O_2 , N_2 , CH_4 , H_2 , H_2O , and CO_2 .
 We assume that reactions proceed to the products of complete combustion
 and apply simple, fast reaction rates according to the following chemical
 equations:



217 These assumptions are not reasonable for the DLR-A flame, but they allow
 218 us to illustrate ODT in a reacting jet configuration with variable properties

219 and heat release, which is the primary purpose of this example case. More
220 complex combustion reaction mechanisms are available within the source
221 code and can be accessed by changing the appropriate input file parameter.

222 This simulation uses ODT parameters $C = 20$, $\beta_{LES} = 17$, and $Z = 400$.
223 The values of C and β_{LES} were adjusted to give good agreement with the
224 experimental data, and the value of Z is the same as it was for the non-
225 reacting jet in Section 3.2. 1024 independent flow realizations were performed
226 in parallel and the results ensemble averaged. Downstream distance y and
227 radial position r are normalized by the jet diameter D .

228 RESULTS AND PLOTS GO HERE

229 4. Impact

230 Questions to answer in this section (from SoftwareX template)

- 231 1. How can new research questions be pursued with this software?
 - 232 • possibility of parametric studies (much harder with DNS/LES/RANS)
 - 233 • study of late-flame soot and radiation interactions, soot emissions
 - 234 as smoke
 - 235 • comparative radiation model studies?
- 236 2. How does the software improve pursuit of existing research questions?
 - 237 • late-flame behavior becomes easier to study
 - 238 • validation of LES subgrid models
 - 239 • soot stuff, especially late in the flame (because soot moves slowly
 - 240 compared to gas species and therefore short simulation times like
 - 241 in DNS aren't enough to study it effectively)
- 242 3. How does the software change the daily practice of its users?
 - 243 • cases take hours or days rather than weeks using supercomputer
 - 244 resources
 - 245 • test cases can be run on local computers (unlike something like
 - 246 DNS) and as background tasks without disrupting other tasks
 - 247 • ODT as a tool complements other approaches, can cover blind
 - 248 spots and be used in validation
- 249 4. How widespread is the software? Who uses it? (Within and outside of
- 250 intended research area and/or group.)
 - 251 • BYU group
 - 252 • JCH at Sandia

- 253 • Chalmers group in Sweden (Marco Fistler, etc.)
- 254 • German university group (Heiko Schmidt, Juan Media, Marten
- 255 Klein, etc.)
- 256 • TO DO: find other groups who have used or currently use ODT
- 257 5. How is the software used in commercial settings (if any)? Has it led to
- 258 creation of spin-off companies?
- 259 • No commercial use (I think).

260 5. Conclusion

261 Write this part next to last

262 6. Conflict of Interest

263 We wish to confirm that there are no known conflicts of interest associated
 264 with this publication and there has been no significant financial support for
 265 this work that could have influenced its outcome.

266 Acknowledgements

267 This work was supported in part by the National Science Foundation
 268 under Grant No. CBET-1403403.

269 References

- 270 [1] D. O. Lignell, G. C. Fredline, A. D. Lewis, Comparison of one-
 271 dimensional turbulence and direct numerical simulations of soot for-
 272 mation and transport in a nonpremixed ethylene jet flame 35 (2) (2015)
 273 1199–1206. doi:10.1016/j.proci.2014.05.046.
- 274 [2] A. W. Abboud, C. Schulz, T. Saad, S. T. Smith, D. D. Harris, D. O.
 275 Lignell, A numerical comparison of precipitating turbulent flows between
 276 large-eddy simulation and one-dimensional turbulence 61 (10) (2015)
 277 3185–3197. doi:10.1002/aic.14870.
- 278 [3] A. R. Kerstein, One-dimensional turbulence: model formulation and ap-
 279 plication to homogeneous turbulence, shear flows, and buoyant stratified
 280 flows 392 (1999) 277–334. doi:10.1017/S0022112099005376.
- 281 [4] A. R. Kerstein, T. D. Dreeben, Prediction of turbulent free shear
 282 flow statistics using a simple stochastic model 12 (2) (2000) 418–424.
 283 doi:10.1063/1.870319.

- 284 [5] A. R. Kerstein, W. T. Ashurst, S. Wunsch, V. Nilsen, One-dimensional
285 turbulence: vector formulation and application to free shear flows 447
286 (2001) 85–109. doi:10.1017/S0022112001005778.
- 287 [6] T. Echekki, A. R. Kerstein, T. D. Dreeben, J.-Y. Chen, ‘one-
288 dimensional turbulence’ simulation of turbulent jet diffusion flames:
289 model formulation and illustrative applications 125 (3) (2001) 1083–
290 1105. doi:10.1016/S0010-2180(01)00228-0.
- 291 [7] J. C. Hewson, A. R. Kerstein, Stochastic simulation of transport and
292 chemical kinetics in turbulent $\text{co}/\text{h}_2/\text{n}_2$ flames 5 (4) (2001) 669–697.
293 doi:10.1088/1364-7830/5/4/309.
- 294 [8] J. C. Hewson, A. R. Kerstein, Local extinction and reignition in
295 nonpremixed turbulent $\text{co}/\text{h}_2/\text{n}_2$ jet flames 174 (5-6) (2002) 35–66.
296 doi:10.1080/713713031.
- 297 [9] D. O. Lignell, D. S. Rappleye, One-dimensional-turbulence simulation
298 of flame extinction and reignition in planar ethylene jet flames 159 (9)
299 (2012) 2930–2943. doi:10.1016/j.combustflame.2012.03.018.
- 300 [10] N. Punati, J. C. Sutherland, A. R. Kerstein, E. R. Hawkes, J. H. Chen,
301 An evaluation of the one-dimensional turbulence model: Comparison
302 with direct numerical simulations of co/h_2 jets with extinction and reig-
303 nition 33 (1) (2011) 1515–1522. doi:10.1016/j.proci.2010.06.127.
- 304 [11] A. Abdelsamie, D. O. Lignell, D. Thévenin, Comparison between
305 odt and dns for ignition occurrence in turbulent premixed jet com-
306 bustion: safety-relevant applications 231 (10) (2017) 1709–1735.
307 doi:10.1515/zpch-2016-0902.
- 308 [12] D. O. Lignell, V. B. Lansinger, A. R. Kerstein, A cylindrical formulation
309 of the one-dimensional turbulence (odt) model for turbulent jet flames,
310 in: AIChE Annual Meeting 2017, American Institute of Chemical En-
311 gineers, 2017.
- 312 [13] B. Goshayeshi, J. C. Sutherland, Prediction of oxy-coal flame stand-off
313 using high-fidelity thermochemical models and the one-dimensional tur-
314 bulence model 35 (3) (2015) 2829–2837. doi:10.1016/j.proci.2014.07.003.
- 315 [14] Z. Jozefik, A. R. Kerstein, H. Schmidt, S. Lyra, H. Kolla, J. H.
316 Chen, One-dimensional turbulence modeling of a turbulent coun-
317 terflow flame with comparison to dns 162 (8) (2015) 2999–3015.
318 doi:10.1016/j.combustflame.2015.05.010.

- [15] E. I. Monson, D. O. Lignell, M. A. Finney, C. Werner, Z. Jozefik, A. R. Kerstein, R. S. Hintze, Simulation of ethylene wall fires using the spatially-evolving one-dimensional turbulence model 52 (1) (2016) 167–196. doi:10.1007/s10694-014-0441-2.
- [16] J. C. Hewson, A. J. Ricks, S. R. Tieszen, A. R. Kerstein, R. O. Fox, Conditional-moment closure with differential diffusion for soot evolution in fire, in: Center for Turbulence Research, Proceedings of the Summer Program 2006, Stanford University, 2006.
- [17] J. C. Hewson, A. J. Ricks, S. R. Tieszen, A. R. Kerstein, R. O. Fox, On the transport of soot relative to a flame: modeling differential diffusion for soot evolution in fire, in: H. Bockhorn, A. D’Anna, A. F. Sarofim, H. Wang (Eds.), Combustion Generated Fine Carbonaceous Particles, KIT Scientific Publishing, 2009, pp. 571–588.
- [18] D. O. Lignell, J. C. Hewson, One-dimensional turbulence simulation: overview and application to soot formation in nonpremixed flames, in: SIAM Conference on Computational Science and Engineering, 2015.
- [19] A. J. Ricks, J. C. Hewson, A. R. Kerstein, J. P. Gore, S. R. Tieszen, W. T. Ashurst, A spatially developing one-dimensional turbulence (odt) study of soot and enthalpy evolution in meter-scale buoyant turbulent flames 182 (1) (2010) 60–101. doi:10.1080/00102200903297003.
- [20] G. Sun, J. C. Hewson, D. O. Lignell, Evaluation of stochastic particle dispersion modeling in turbulent round jets 89 (2017) 108–122. doi:10.1016/j.ijmultiphaseflow.2016.10.005.
- [21] J. R. Schmidt, J. O. L. Wendt, A. R. Kerstein, Non-equilibrium wall deposition of inertial particles in turbulent flow 137 (2) (2009) 233–257. doi:10.1007/s10955-009-9844-8.
- [22] G. Sun, D. O. Lignell, J. C. Hewson, C. R. Gin, Particle dispersion in homogeneous turbulence using the one-dimensional turbulence model 26 (10) (2014) 103301. doi:10.1063/1.4896555.
- [23] M. Fistler, D. O. Lignell, A. R. Kerstein, M. Oevermann, Numerical studies of turbulent particle-laden jets using spatial approach of one-dimensional turbulence, in: ILASS-Europe 28th Conference on Liquid Atomization and Spray Systems, 2017.
- [24] S. Cao, T. Echehki, A low-dimensional stochastic closure model for combustion large-eddy simulation 9. doi:10.1080/14685240701790714.

- [25] R. C. Schmidt, A. R. Kerstein, S. Wunsch, V. Nilsen, Near-wall les closure based on one-dimensional turbulence modeling 186 (1) (2003) 317–355. doi:10.1016/S0021-9991(03)00071-8.
- [26] R. C. Schmidt, A. R. Kerstein, R. McDermott, Odtles: A multi-scale model for 3d turbulent flow based on one-dimensional turbulence modeling 199 (13-16) (2010) 865–880. doi:10.1016/j.cma.2008.05.028.
- [27] E. Gonzalez-Juez, A. R. Kerstein, D. O. Lignell, Fluxes across double-diffusive interfaces: a one-dimensional-turbulence study 677 (2011) 218–254. doi:10.1017/jfm.2011.78.
- [28] E. Gonzalez-Juez, A. R. Kerstein, D. O. Lignell, Reactive rayleigh–taylor turbulent mixing: a one-dimensional-turbulence study 107 (5) (2013) 506–525. doi:10.1080/03091929.2012.736504.
- [29] S. Wunsch, A. R. Kerstein, A model for layer formation in stably stratified turbulence 13 (3) (2001) 702–712. doi:10.1063/1.1344182.
- [30] D. O. Lignell, V. B. Lansinger, J. Medina, M. Klein, A. R. Kerstein, H. Schmidt, M. Fistler, M. Oevermann, One-dimensional turbulence modeling for cylindrical and spherical flows: model formulation and application 32 (4) (2018) 495–520. doi:10.1007/s00162-018-0465-1.
- [31] M. Klein, D. O. Lignell, H. Schmidt, Map-based modeling of turbulent convection: Application of the one-dimensional turbulence model to planar and spherical geometries, in: International Conference on Rayleigh-Benard Turbulence, 2018.
- [32] M. Klein, D. O. Lignell, H. Schmidt, Stochastic modeling of temperature and velocity statistics in spherical-shell convection, in: EGU Conference on Recent developments in Geophysical Fluid Dynamics, 2019.
- [33] W. T. Ashurst, A. R. Kerstein, One-dimensional turbulence: Variable-density formulation and application to mixing layers 17 (2). doi:10.1063/1.1847413.
- [34] D. O. Lignell, A. R. Kerstein, G. Sun, E. I. Monson, Mesh adaption for efficient multiscale implementation of one-dimensional turbulence 27 (3-4) (2013) 273–295. doi:10.1007/s00162-012-0267-9.
- [35] Y. A. Çengel, J. M. Cimbala, Fluid Mechanics, 2nd Edition, Çengel series in engineering thermal-fluid sciences, McGraw-Hill Higher Education, 2010.

- 388 [36] J. Beder, yaml-cpp v0.6.3 (2008).
 389 URL <https://github.com/jbeder/yaml-cpp/>
- 390 [37] A. C. Hindmarsh, R. Serban, D. R. Reynolds, CVODE,
 391 https://computing.llnl.gov/sites/default/files/public/cv_guide.pdf
 392 (2020).
 393 URL <https://computing.llnl.gov/projects/sundials/cvode>
- 394 [38] G. Strang, On the construction and comparison of difference schemes
 395 5 (3) (1968) 506–517. doi:10.1137/0705041.
- 396 [39] D. G. Goodwin, R. L. Speth, H. K. Moffat, B. W. Weber, Cantera
 397 (2018). doi:10.5281/zenodo.1174508.
 398 URL <https://cantera.org/>
- 399 [40] D. van Heesch, Doxygen (2018).
 400 URL <https://www.doxygen.nl/>
- 401 [41] G. K. El Khoury, P. Schlatter, A. Noorani, P. F. Fischer, G. Brethouwer,
 402 A. V. Johansson, Direct numerical simulation of turbulent pipe
 403 flow at moderately high reynolds numbers 91 (3) (2013) 475–495.
 404 doi:10.1007/s10494-013-9482-8.
- 405 [42] C. Chin, J. P. Monty, A. Ooi, Reynolds number effects in dns of pipe
 406 flow and comparison with channels and boundary layers 45 (2014) 33–40.
 407 doi:10.1016/j.ijheatfluidflow.2013.11.007.
- 408 [43] H. J. Hussein, S. P. Capp, W. K. George, Velocity measurements in a
 409 high-reynolds-number, momentum-conserving, axisymmetric, turbulent
 410 jet 258 (1994) 31–75. doi:10.1017/S002211209400323X.
- 411 [44] W. Meier, R. S. Barlow, Y.-L. Chen, J.-Y. Chen, Raman/Rayleigh/LIF
 412 measurements in a turbulent CH₄/H₂/N₂ jet diffusion flame: experi-
 413 mental techniques and turbulence–chemistry interaction 123 (3) (2000)
 414 326–343. doi:10.1016/S0010-2180(00)00171-1.
 415 URL <https://tnfworkshop.org/data-archives/simplejet/dlrflames/>
- 416 [45] H. Pitsch, Unsteady flamelet modeling of differential diffusion in tur-
 417 bulent jet diffusion flames 123 (3) (2000) 358–374. doi:10.1016/S0010-
 418 2180(00)00135-8.
- 419 [46] R. P. Lindstedt, H. Ozarovsky, Joint scalar transported pdf model-
 420 ing of nonpiloted turbulent diffusion flames 143 (4) (2005) 471–490.
 421 doi:10.1016/j.combustflame.2005.08.030.

- 422 [47] H. Wang, S. B. Pope, Large eddy simulation/probability density func-
 423 tion modeling of a turbulent $\text{CH}_4/\text{H}_2/\text{N}_2$ jet flame 33 (1) (2011) 1319–1330.
 424 doi:10.1016/j.proci.2010.08.004.
- 425 [48] M. Fairweather, R. M. Woolley, First-order conditional moment closure
 426 modeling of turbulent, nonpremixed methane flames 138 (1-2) (2004)
 427 3–19. doi:10.1016/j.combustflame.2004.03.001.
- 428 [49] K. W. Lee, D. H. Choi, Prediction of NO in turbulent diffusion
 429 flames using eulerian particle flamelet model 12 (5) (2008) 905–927.
 430 doi:10.1080/13647830802094351.
- 431 [50] K. W. Lee, D. H. Choi, Analysis of NO formation in high
 432 temperature diluted air combustion in a coaxial jet flame us-
 433 ing an unsteady flamelet model 52 (5-6) (2009) 1412–1420.
 434 doi:10.1016/j.ijheatmasstransfer.2008.08.015.

435 **Current executable software version**

436 Ancillary data table required for sub version of the executable software:
 437 (x.1, x.2 etc.) kindly replace examples in right column with the correct
 438 information about your executables, and leave the left column as it is.

Nr.	(Executable) software meta-data description	Please fill in this column
S1	Current software version	2.1
S2	Permanent link to executables of this version	For example: <i>https</i> : <i>//github.com/combogenomics/DuctApe/releases/tag/DuctApe - 0.16.4</i>
S3	Legal Software License	MIT
S4	Computing platforms/Operating Systems	Linux, OS X, Microsoft Windows
S5	Installation requirements & dependencies	CMake 3.12+, Cantera, Git, Doxygen (optional)
S6	If available, link to user manual - if formally published include a reference to the publication in the reference list	For example: <i>http</i> : <i>//mozart.github.io/documentation/</i>
S7	Support email for questions	davidlignell@byu.edu

Table 2: Software metadata (optional)